

New Ru^{II}Rh^{III} Bimetallic Motif with a Single Rh-Cl Bond as a Supramolecular Photocatalyst for Proton Reduction

Rongwei Zhou, Gerald F. Manbeck, Dexter G. Wimer, and Karen J. Brewer*

Department of Chemistry, Virginia Tech, 306 Hahn Hall, Blacksburg, Virginia 24060-0212,
United States.

Email: rowezhou@vt.edu

Supporting Information

Table of contents

Experimental section	S3-S6
Fig. S1: Synthetic scheme	S7
Fig. S2: ^1H NMR spectra of $[\text{Ru}^{\text{II}}\text{Rh}^{\text{III}}\text{Cl}(\text{tpy})]^{4+}$ and its deuterated versions	S8
Fig. S3: ^1H NMR spectra of $[\text{Ru}^{\text{II}}\text{Rh}^{\text{III}}\text{Cl}_2(\text{bpy})]^{3+}$ and its deuterated versions	S19
Fig. S4: CVs of $[\text{Ru}^{\text{II}}\text{Rh}^{\text{III}}\text{Cl}(\text{tpy})]^{4+}$ and its reduction product	S10
Fig. S5: CVs of $\text{Rh}^{\text{III/II}}$ reduction at different scan rates	S10
Fig. S6: Electronic absorption spectrum	S10
Fig. S7: Emission spectra	S11
Fig. S8: Electronic absorption spectrum with electrochemical reduction	S11
Fig. S9: Hydrogen production profile of $[\text{Ru}^{\text{II}}\text{Rh}^{\text{III}}\text{Cl}_2(\text{bpy})]^{3+}$	S12
Fig. S10: Hydrogen production profile of $[\{(\text{bpy})_2\text{Ru}(\text{dpp})\}_2\text{RhCl}_2]^{5+}$	S12
Fig. S11: CVs of $[\text{Ru}^{\text{II}}\text{Rh}^{\text{III}}\text{Cl}_2(\text{bpy})]^{3+}$ and its reduction product.	S13
Fig. S12: ESI mass spectrum of the reduction product of $[\text{Ru}^{\text{II}}\text{Rh}^{\text{III}}\text{Cl}_2(\text{bpy})]^{3+}$.	S13
Fig. S13: CVs of $[\text{Rh}^{\text{III}}\text{Cl}(\text{dpp})(\text{tpy})]^{2+}$ and its reduction product.	S14
Fig. S14: ESI mass spectrum of the reduction product of $[\text{Rh}^{\text{III}}\text{Cl}(\text{dpp})(\text{tpy})]^{2+}$	S14
Fig. S15: Hydrogen production profile of $[\text{RuRhCl}(\text{tpy})]^{4+}$ with addition of 1.eq of tpy or Cl^-.	S15
Table S1: Photophysical data	S15
Table S2: Photocatalytic hydrogen production data	S16
Quantum Efficiency Sample Calculation	S16
References	S16

Experimental Section

Materials. All chemicals and solvents were used as received unless otherwise stated. Acetonitrile was distilled from CaH₂. RhCl₃·3H₂O was purchased from Strem Chemicals. Sephadex LH-20 was purchased from GE Healthcare Biosciences Corporation. bpy, tpy and DMA were purchased from Sigma Aldrich. The complex [(bpy)₂Ru(dpp)](PF₆)₂ was prepared as reported.¹ Deuterated ligands, *d*₁₀-dpp, *d*₈-bpy, and *d*₁₁-tpy, and bimetallic Ru^{II}Rh^{III} with deuterated ligands were prepared as reported.^{2,3} ¹H NMR and ¹H-¹H COSY spectra were recorded on Varian MR 400 MHz instrument. Elemental analysis was conducted in Atlantic Microlab, Inc.

Synthesis of [RhCl₃(bpy)(DMF)]. To 3 mL of DMF (*N,N*-dimethylformamide) containing RhCl₃·3H₂O (0.10 g, 0.38 mmol), bpy (0.06 g, 0.38 mmol) was added. The mixture was heated at 65 °C for 3 h, during which the initial suspension turned into an orange solution. After cooling, diethyl ether (*ca.* 20 mL) was added to induce precipitation. The precipitate was filtered, washed sequentially with H₂O (*ca.* 10 mL), ethanol (*ca.* 10 mL), and diethyl ether (*ca.* 10 mL), and dried under vacuum with a yield of 75% (0.14 g, 0.30 mmol). ¹H NMR (400 MHz, ppm, CD₃Cl): δ 9.99 (d, 1H), 9.11 (d, 1H), 8.65 (s, 1H, DMF), 8.10 (dt, *J* = 6.2, 6.6 Hz, 4H), 7.68 (t, *J* = 7.0 Hz, 1H), 7.58 (t, *J* = 7.7 Hz, 1H). 3.23 (s, 3H, DMF), 3.19 (s, 3H, DMF). ESI-MS: [M+NH₄]⁺ *m/z*, *Found* = 454.9, *Calc'd* = 454.9.

Synthesis of [RhCl₃(tpy)]. A mixture of RhCl₃·3H₂O (0.10 g, 0.38 mmol) and tpy (0.09 g, 0.38 mmol) in 15 mL methanol was heated at reflux for 3 h. After cooling, the yellow precipitate was collected and washed with H₂O (*ca.* 10 mL), ethanol (*ca.* 10 mL), and diethyl ether (*ca.* 10 mL). The collected solid was dried in the oven at 100 °C, with a yield of 90% (0.15 g, 0.34 mmol). ¹H NMR (400 MHz, ppm, DMSO-*D*₆): δ 9.28 (d, *J* = 5.6 Hz, 2H), 8.82 (d, *J* = 7.9 Hz, 2H), 8.78 (d, *J* = 8.0 Hz, 2H), 8.55 (t, *J* = 8.1 Hz, 1H), 8.39 (m, 2H), 7.96 (m, 2H), ESI-MS: [M+NH₄]⁺ *m/z*, *Found* = 458.9, *Calc'd* = 458.9.

Synthesis of [(bpy)₂Ru(dpp)RhCl₂(bpy)](PF₆)₃. [(bpy)₂Ru(dpp)](PF₆)₂ (0.18 g, 0.20 mmol) and [RhCl₃(bpy)(DMF)] (0.08 g, 0.19 mmol) were heated at reflux in 10 mL of ethanol/water (1:1, v/v) for 1.5 h and afforded a purple solution. The solution was cooled to room temperature and added dropwise into a saturated KPF₆ aqueous solution (*ca.* 50 mL) to induce precipitation.

The purple precipitate was filtered and washed with water (2×10 mL), ethanol (2×10 mL), and diethyl ether (2×10 mL). The crude product was purified by LH-20 size exclusion chromatography column using ethanol/acetonitrile (2:1, v/v) as the mobile phase. The first purple band was collected and solvent was removed by rotary evaporation. The resulting solid was dissolved in a minimal amount of acetone and re-precipitated by adding diethyl ether. A purple solid was collected and dried under vacuum with a yield of 50% (0.13 g, 0.10 mmol). ESI-MS: $[M-PF_6]^+$ m/z , *Found* = 1266.9, *Calc'd* = 1266.9.

Synthesis of $[(bpy)_2Ru(dpp)RhCl(tpy)](PF_6)_4$. $[(bpy)_2Ru(dpp)RhCl(tpy)](PF_6)_4$ was prepared in a similar manner as $[(bpy)_2Ru(dpp)RhCl_2(bpy)](PF_6)_3$ by refluxing the mixture of $[(bpy)_2Ru(dpp)](PF_6)_2$ (0.27 g, 0.30 mmol) and $[RhCl_3(tpy)]$ (0.12 g, 0.30 mmol) in ethanol/water (1:3, v/v). After purification, 0.16 g purple solid (0.10 mmol) was obtained in 30% yield. *Anal. Calc'd.* for $C_{49}H_{37}N_{11}RuRhClP_4F_{24}$, C, 9.63; H, 2.33; N, 36.80; *Found:* C, 9.54; H, 2.61; N, 36.77. ESI-MS: $[M-PF_6]^+$, m/z , *Found* = 1453.9, *Calc'd* = 1453.9; $[M - 2PF_6]^{2+}$ m/z , *Found* = 654.5, *Calc'd* = 654.5.

Synthesis of $[RhCl(dpp)(tpy)](PF_6)_2$. $[RhCl_3(tpy)]$ (0.17, 0.40 mmol) and dpp (0.09 g, 0.40 mmol) were heated at reflux in 10 mL of ethanol/water (1:1, v/v) for 4 h to afford a light yellow solution. The solution was cooled to room temperature and added dropwise into 50 mL saturated KPF_6 aqueous solution to induce precipitation. The light yellow powder was filtered and washed with water (*ca.* 20 mL), ethanol (*ca.* 10 mL), and diethyl ether (*ca.* 20 mL). Yield: 0.28 g, 0.30 mmol, 70%, ESI-MS: $[M + Na]^+$, m/z , *Found* = 917.9, *Calc'd* = 917.9.

Electrochemistry. Cyclic voltammetry experiments were conducted using a Bioanalytical Systems (BAS) electrochemical analyzer and a three-electrode cell. All measurements were performed at room temperature under Ar with a Pt disk working electrode, a Pt wire auxiliary electrode, and an Ag/AgCl reference electrode in 0.1 M Bu_4NPF_6 acetonitrile ($FeCp_2^+/FeCp_2 = 0.44$ V vs Ag/AgCl) solution with a scan rate of $0.1 V \cdot s^{-1}$. Bulk electrolysis was performed with a carbon cloth working electrode and an Ag/AgCl reference electrode in 0.1 M Bu_4NPF_6 acetonitrile solution. A Pt coil counter electrode was held in a tube filled with 0.1 M Bu_4NPF_6 acetonitrile solution and separated from the working solution by a porous vycor® glass tip. The solution was continuously bubbled with Ar during the bulk electrolysis. Cyclic voltammetry was

used to monitor the progress of electrolysis. The charge passed during bulk electrolysis was calculated from current decay curves (i vs t) by subtracting the charge from capacitive current.

Electronic Absorption Spectroscopy. Electronic absorption spectra were recorded in a Hewlett Packard 8452A diode array spectrophotometer, measuring from 190 nm to 1100 nm with a sampling interval of 2 nm and an integration time of 0.5 s. All spectra were collected in UV-grade acetonitrile using a 1 cm path length quartz cuvette at room temperature (Starna Cells, Inc.; Atascadero, CA). Extinction coefficient measurements were performed in triplicate.

Emission Spectroscopy. Emission spectra were measured in degassed UV-grade acetonitrile using a 1 cm path length quartz cuvette and a QuantaMaster Model QM-200-45E fluorimeter from Photon Technologies International, Inc. Samples were excited by a water-cooled 150 W Xenon arc lamp, with the corresponding emission collected at a 90° angle using a thermoelectrically cooled Hamamatsu 1527 photomultiplier tube operating in a photon counting mode with 0.25 nm resolution. The emission quantum yields for all samples were measured with the same instrumental settings and were referenced to $[\text{Os}(\text{bpy})_3]^{2+}$ ($\Phi^{\text{em}} = 4.62 \times 10^{-3}$).⁴ For 77 K emission spectra, all samples were prepared in an ethanol/methanol (4:1,v/v) solution and submerged in liquid N₂ in a finger dewar to form a transparent rigid glass matrix. All emission spectra were corrected for PMT response.

Excited State Lifetime Measurements. Excited state lifetimes were collected on a Photon Technologies International, Inc. PL-2300 nitrogen laser with a PL-201 tunable dye laser as an excitation source (360 nm – 900 nm). Dye coumarin 500 was used and excitation monochromator was set to 520 nm. The emission was collected using a Hamamatsu R928 photomultiplier tube operating at a 90° angle from the excitation source after passing through an emission monochromator. The signal was recorded using a LeCroy 9361 dual 300 MHz oscilloscope which averaged the results of 300 sweeps. A single exponential function, $Y = A + Be^{-x/\tau}$ (τ is lifetime in seconds) was fit to all data profiles. All complexes were studied with the same instrument settings.

Photocatalytic H₂ Production. Photocatalytic hydrogen production of $[(\text{bpy})_2\text{Ru}(\text{dpp})\text{RhCl}(\text{tpy})](\text{PF}_6)_4$ and $[(\text{bpy})_2\text{Ru}(\text{dpp})\text{RhCl}_2(\text{bpy})](\text{PF}_6)_3$ were carried out using the previously reported conditions.⁵ The mixture of solvent (acetonitrile, DMF or acetone), bimetallic complex, and deionized water was purged with Ar in reaction vessels capped with air

tight septa. Separately Ar-purged DMA was added to the reaction vessels just prior to photolysis (65 μM metallic complex, 1.5 M DMA, and 0.6 M deionized water in 4.5 mL solution). A home-made 470 nm LED light source array with 0.2 W output irradiates from the bottom of the vessels (light flux $(2.36 \pm 0.05 \times 10^{19})$ photons/min). A HY-OPTIMATM 700 in-line process solid state hydrogen sensor from H2scan was equipped on the top of photolysis vessels to measure hydrogen production in real-time. The amount of hydrogen was calibrated using a calibration curve. Production of H₂ was verified by GC analysis after photolysis. The reported value for hydrogen production is the average of three experiments.

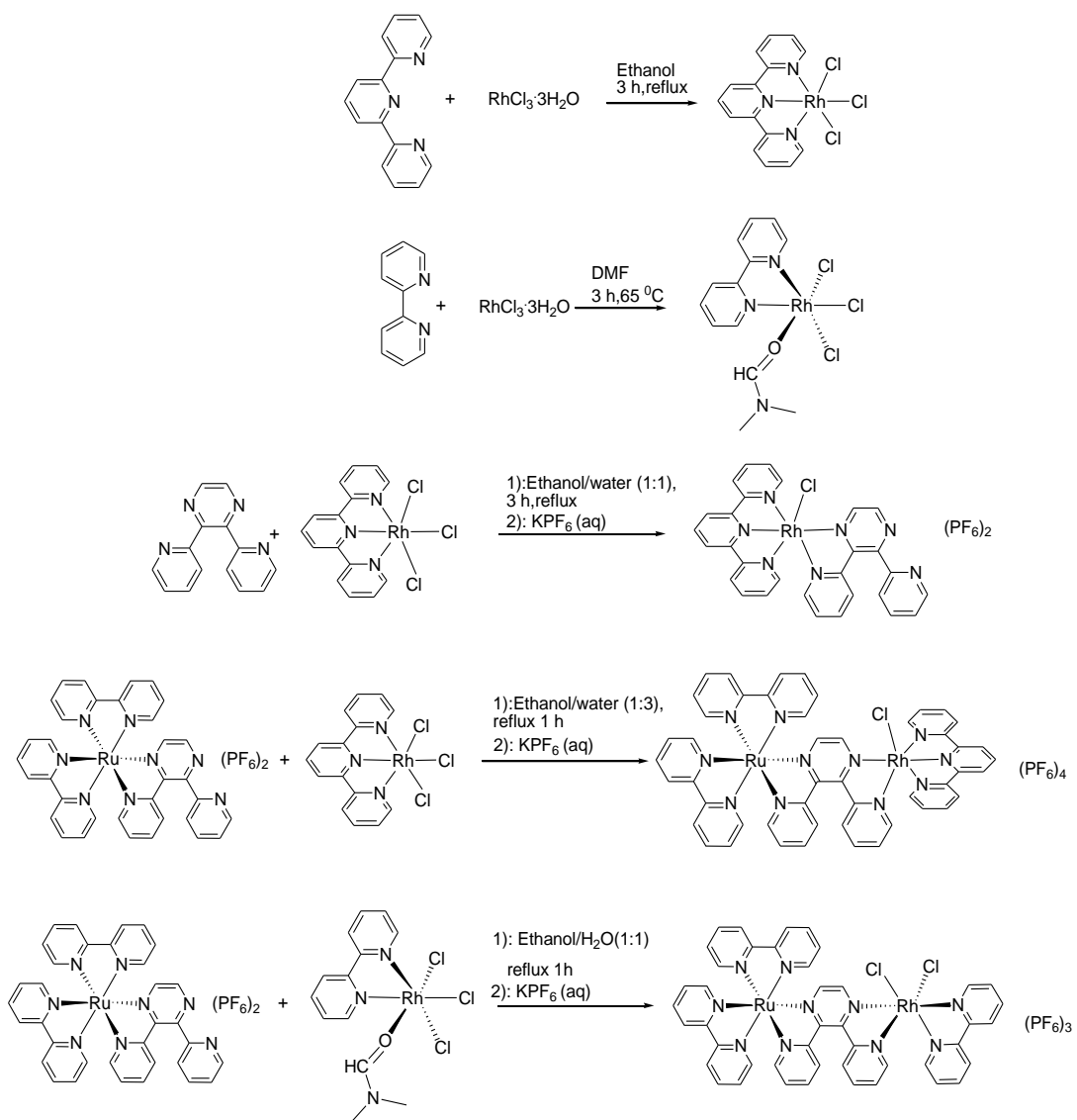


Fig. S1: Synthesis of Rh monometallics and Ru(II),Rh(III) bimetallics.

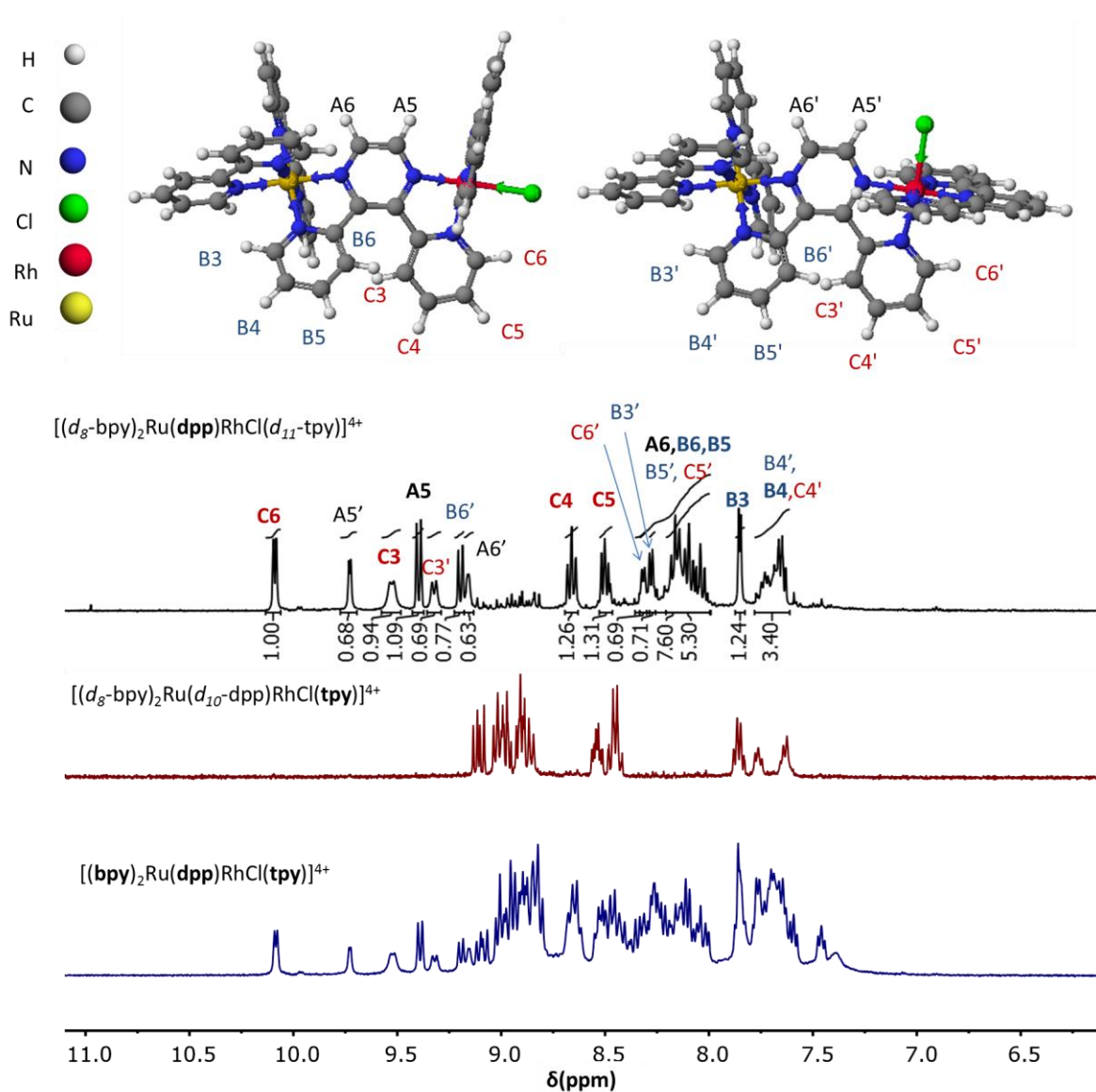


Fig. S2 : (top): MM2 minimized three-dimensional structures (Scigrass 7.7.1 molecular modeling) software of two geometric isomers of $[(\text{bpy})_2\text{Ru}(\text{dpp})\text{RhCl}(\text{tpy})](\text{PF}_6)_4$ with the number labeling the dpp protons and ^1H NMR spectrum; (bottom): ^1H NMR spectra of $[(d_8\text{-bpy})_2\text{Ru}(\text{dpp})\text{RhCl}(d_{11}\text{-tpy})](\text{PF}_6)_4$, $[(d_8\text{-bpy})_2\text{Ru}(d_{10}\text{-dpp})\text{RhCl}(\text{tpy})](\text{PF}_6)_4$ and $[(\text{bpy})_2\text{Ru}(\text{dpp})\text{RhCl}(\text{tpy})](\text{PF}_6)_4$ (bpy = 2,2'-bipyridine, dpp = 2,3-bis(2-pyridyl)pyrazine, tpy = 2,2':6',2''-terpyridine) at 22 °C in d_6 -acetone.³

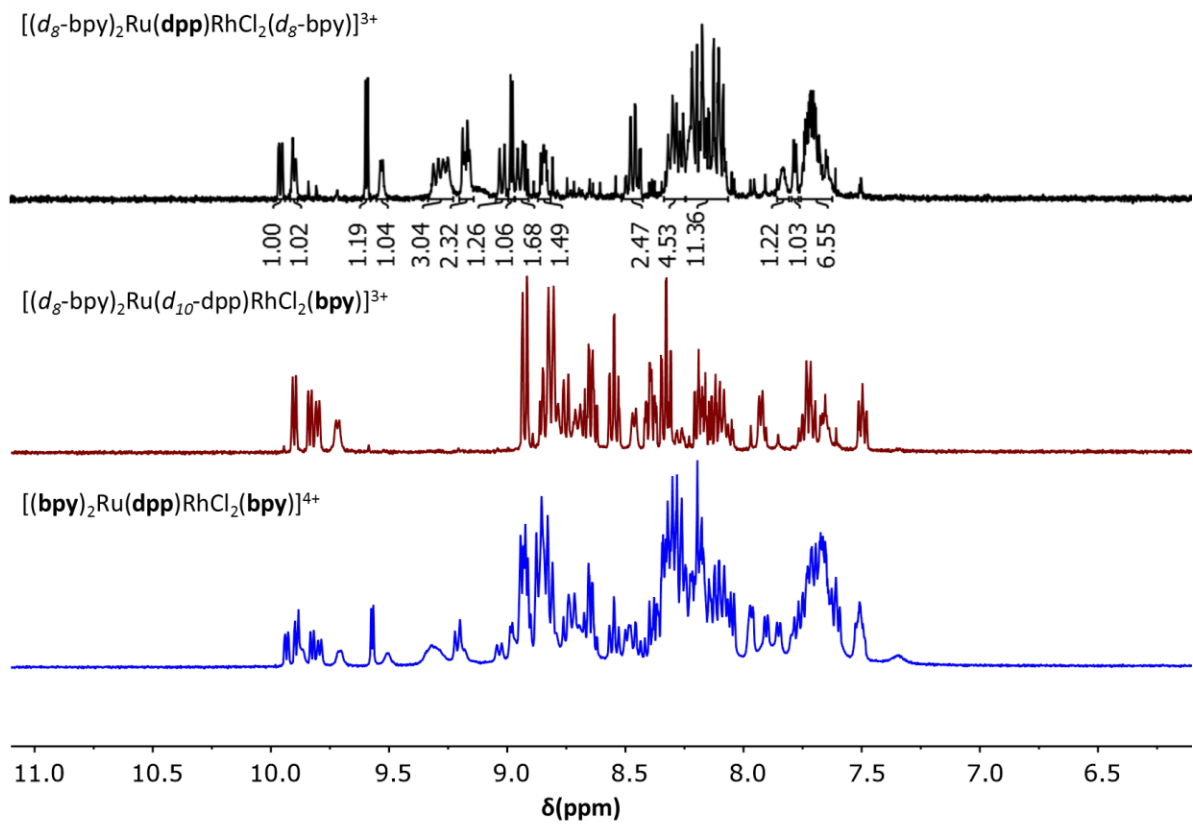


Fig. S3: ^1H NMR spectra of $[(d_8\text{-bpy})_2\text{Ru}(\text{dpp})\text{RhCl}_2(d_8\text{-bpy})](\text{PF}_6)_3$, $[(d_8\text{-bpy})_2\text{Ru}(d_{10}\text{-dpp})\text{RhCl}_2(\text{bpy})](\text{PF}_6)_3$ and $[(\text{bpy})_2\text{Ru}(\text{dpp})\text{RhCl}_2(\text{bpy})](\text{PF}_6)_3$ (bpy = 2,2'-bipyridine, dpp = 2,3-bis(2-pyridyl)pyrazine, tpy = 2,2':6',2''-terpyridine) at 22 °C in d_6 -acetone.³

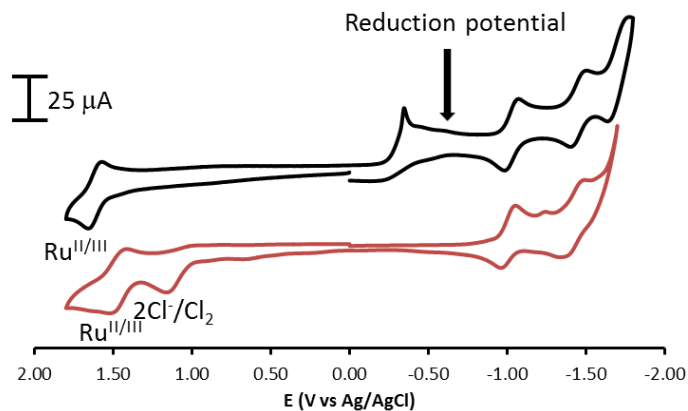


Fig. S4: Cyclic voltammograms before (black) and after (red) control potential electrolysis of $[(bpy)_2Ru(dpp)RhCl(tpy)]^{4+}$ at -0.65 V with scan rate of 100 $mV s^{-1}$ in 0.1 M Bu_4NPF_6 CH_3CN solution. Two equivalents of charge were passed during electrolysis.

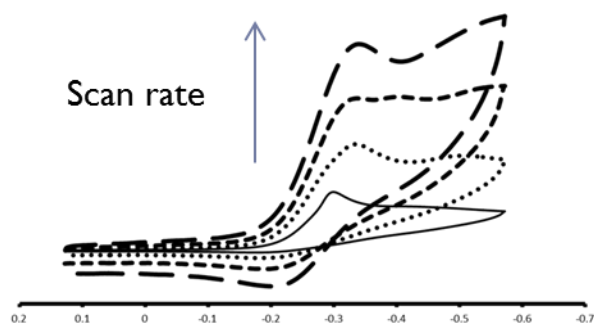


Fig. S5: Cyclic voltammograms of $Rh^{III/II/I}$ reduction couple of $[(bpy)_2Ru(dpp)RhCl(tpy)](PF_6)_4$ with the scan rate varied from 100 $mV s^{-1}$ to 1000 $mV s^{-1}$

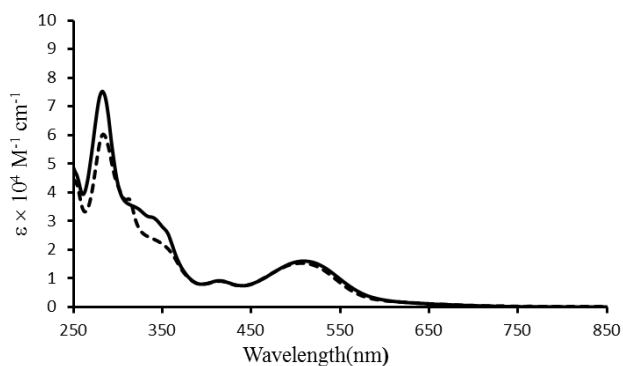


Fig. S6: Electronic absorption spectra of $[(bpy)_2Ru(dpp)Cl_2(bpy)](PF_6)_3$ (--) and $[(bpy)_2Ru(dpp)Cl(tpy)](PF_6)_3$ (—) at room temperature in acetonitrile (bpy = 2,2'-bipyridine, dpp = 2,3-bis(2-pyridyl)pyrazine, tpy = 2,2':6',2''-terpyridine).

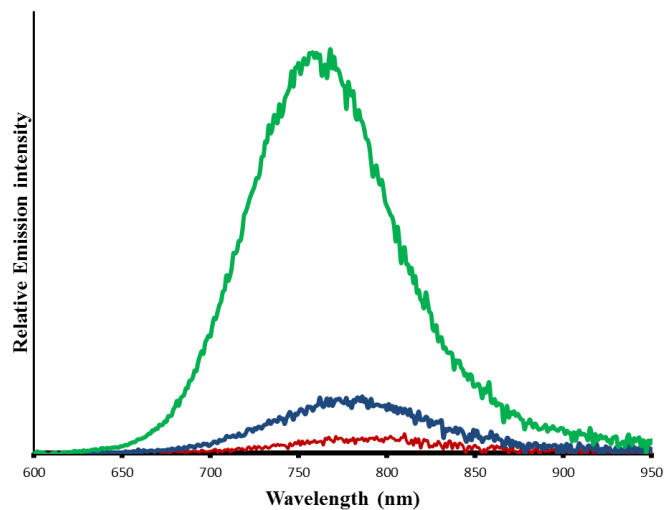


Fig. S7: Emission spectra of $[\{(bpy)_2Ru\}_2(dpp)]^{4+}$ (green), $[(bpy)_2Ru(dpp)Cl_2(bpy)]^{3+}$ (blue) and $[(bpy)_2Ru(dpp)Cl(tpy)]^{4+}$ (red) at room temperature in acetonitrile.

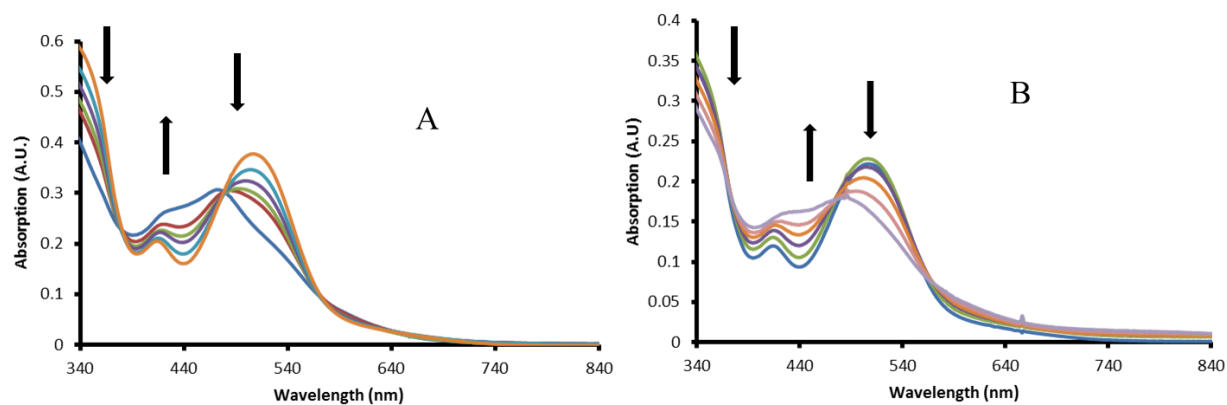


Fig. S8: Electronic absorption spectra generated from electrochemical reduction at -0.95 V vs Ag/AgCl (A) and photochemical reduction (B) of $[(bpy)_2Ru(dpp)RhCl_2(bpy)](PF_6)_3$ in deoxygenated acetonitrile at room temperature.

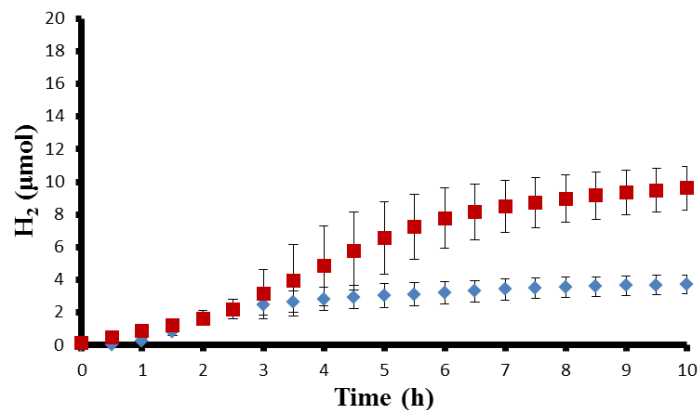


Figure S9: Photocatalytic hydrogen production of $[(bpy)_2Ru(dpp)RhCl_2(bpy)](PF_6)_3$ ($65 \mu M$) in CH_3CN (blue diamonds) and DMF (red squares) with 1.5 M DMA and 0.6 M H_2O under 470 nm LED light irradiation.

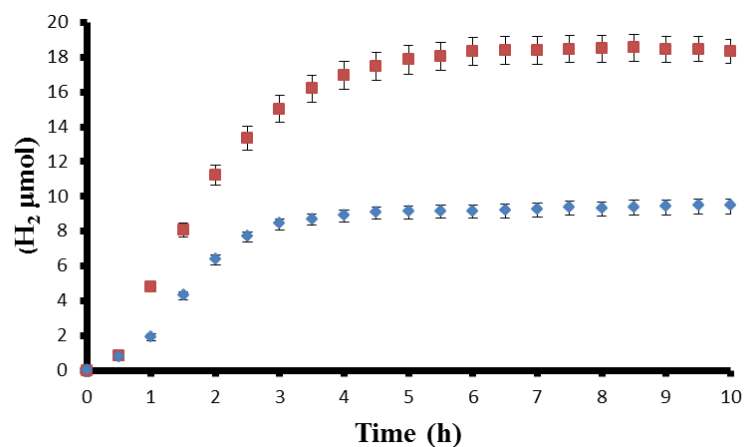


Figure S10: Photocatalytic hydrogen production of $[\{ (bpy)_2Ru(dpp) \} RhCl_2] (PF_6)_5$ ($65 \mu M$) in CH_3CN (blue diamonds) and DMF (red squares) with 1.5 M DMA and 0.6 M H_2O under 470 nm LED light irradiation.

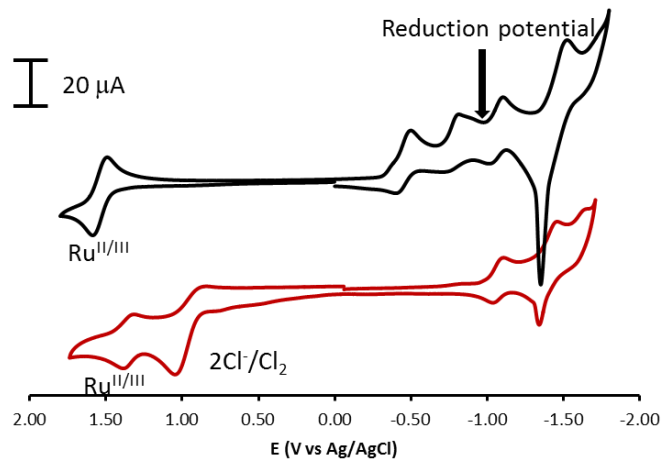


Fig. S11: Cyclic voltammograms before (black) and after (red) control potential electrolysis of $[(\text{bpy})_2\text{Ru}^{\text{II}}(\text{dpp})\text{Rh}^{\text{III}}\text{Cl}_2(\text{bpy})]^{3+}$ at -0.95 V with a scan rate of 100 mV s^{-1} in 0.1 M Bu_4NPF_6 CH_3CN solution. Two equivalents of charge were passed during electrolysis.

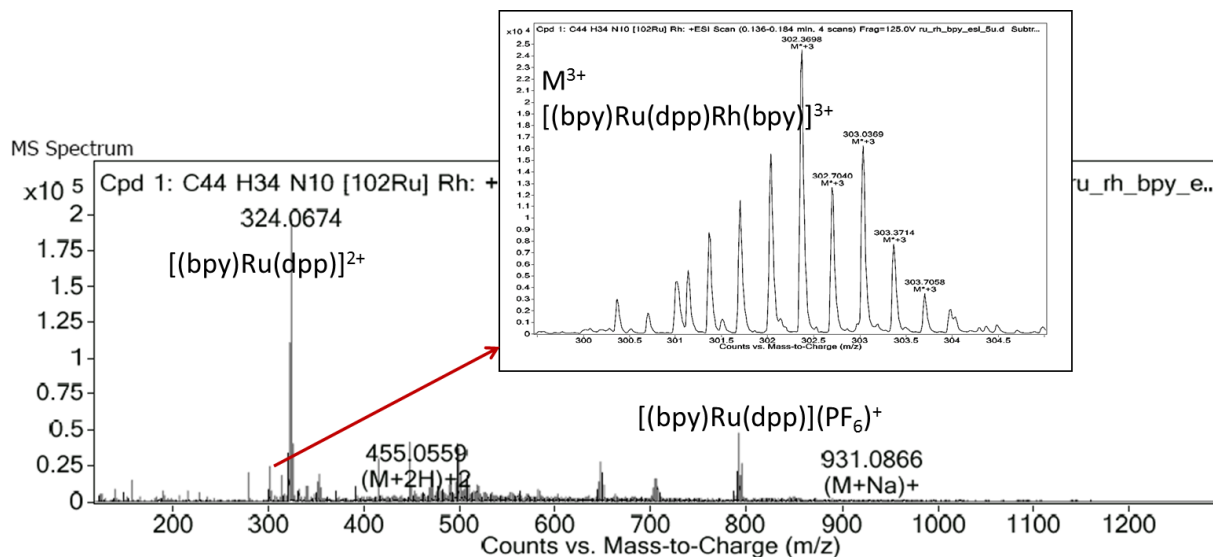


Fig. S12: ESI mass spectrum of product after two-electron reduction of $[(\text{bpy})_2\text{Ru}^{\text{II}}(\text{dpp})\text{Rh}^{\text{III}}\text{Cl}_2(\text{bpy})]^{3+}$ by control potential electrolysis showing the formation of $[(\text{bpy})_2\text{Ru}^{\text{II}}(\text{dpp})\text{Rh}^{\text{I}}(\text{bpy})]^{3+}$.

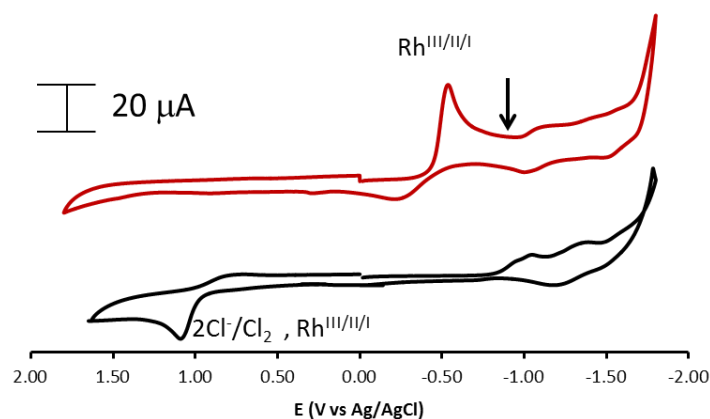


Fig. S13: Cyclic voltammogram before (black) and after (red) control potential electrolysis of $[\text{RhCl}(\text{dpp})(\text{tpy})]^{2+}$ at -0.80 V with a scan rate of 100 mV/s in 0.1 M Bu_4NPF_6 CH_3CN solution. Two equivalents of charge were passed in the electrolysis.

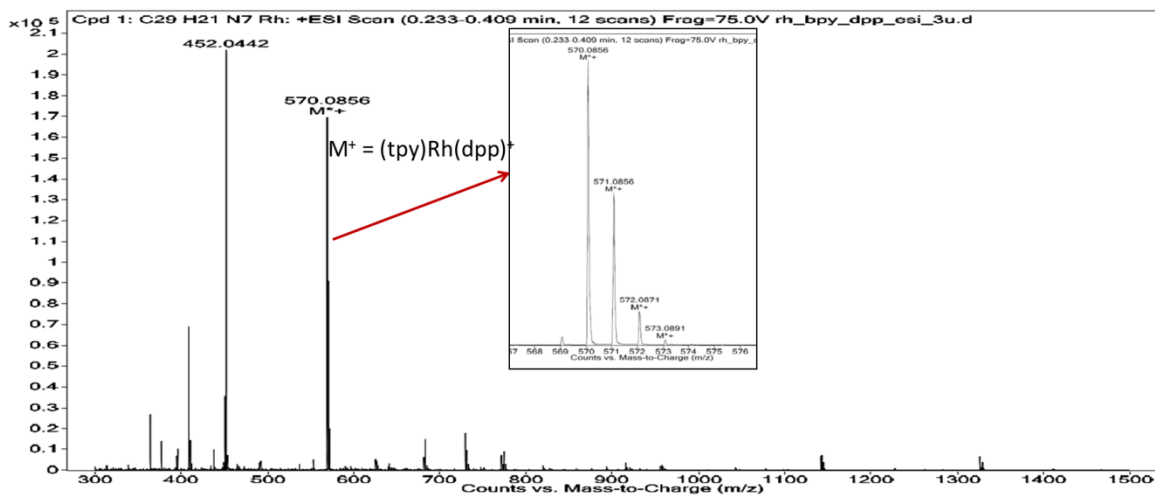


Fig. S14: ESI mass spectrum of product after control potential electrolysis of $[\text{Rh}^{\text{III}}\text{Cl}(\text{dpp})(\text{tpy})]^{2+}$ showing the formation of $[(\text{dpp})\text{Rh}^{\text{I}}(\text{bpy})]^+$.

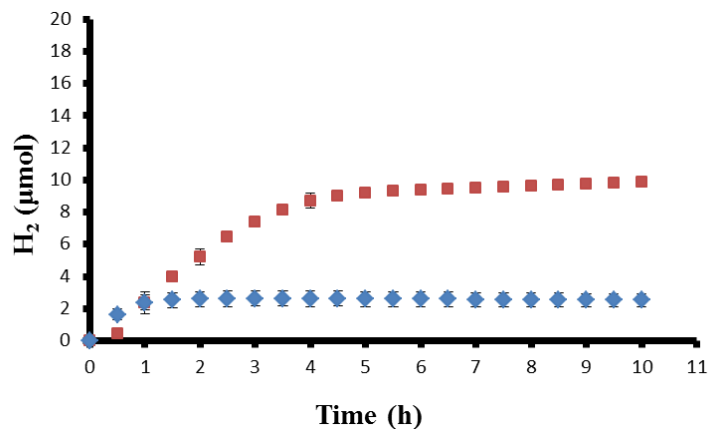


Figure S15: Photocatalytic hydrogen production of $[(\text{bpy})_2\text{Ru}(\text{dpp})\text{RhCl}(\text{tpy})](\text{PF}_6)_4$ ($65 \mu\text{M}$) in CH_3CN under 470 nm LED light irradiation with 1.5 M DMA, 0.6 M H_2O and $65 \mu\text{M}$ Bu_4NCl (blue diamond) or $65 \mu\text{M}$ tpy (red square).

Table S1: Photophysical properties of Ru(II),Rh(III) supramolecular complexes

Complex ^a	RT				77 K ^c	
	λ^{em} (nm)	$\Phi \times 10^4$	τ (ns)	$k_{\text{et}} \times 10^{-7}$	λ^{em} (nm)	τ (μs)
$[(\text{bpy})_2\text{Ru}(\text{dpp})\text{RhCl}(\text{tpy})]^{4+}$	780	0.65	30	2.6	715	2.1
$[(\text{bpy})_2\text{Ru}(\text{dpp})\text{RhCl}_2(\text{bpy})]^{3+}$	775	1.3	40	1.7	715	2.3
$[(\text{bpy})_2\text{Ru}(\text{dpp})\text{RhCl}_2(\text{phen})]^{3+}$	770	1.2	30	1.5	715	1.8
$[\{(\text{bpy})_2\text{Ru}(\text{dpp})\}_2\text{RhCl}_2]^{5+ d}$	776	2.6	38	1.9	730	1.9
$[\{(\text{bpy})_2\text{Ru}\}_2(\text{dpp})](\text{PF}_6)_4$	758	8.9	130		695	2.4

^a bpy = 2,2'-bipyridine, dpp = 2,3-bis(2-pyridyl)pyrazine, and tpy = 2,2':6',2''- terpyridine. ^b data were measured in room temperature acetonitrile and corrected for PMT response. ^c 77 K emission data were collected in ethanol/methanol (4:1 v/v) glass and corrected for PMT response. ^d from ref. 4⁶

Table S2: Photocatalytic hydrogen production.

Complex	Solvent	H ₂ (μmol) ^a	TON ^b
Ru ^{II} Rh ^{III} Cl(tpy) ⁴⁺	CH ₃ CN	9.8 ± 0.6	33 ± 2
	acetone	17 ± 1.4	58 ± 5
	DMF	17 ± 0.9	58 ± 3
Ru ^{II} Rh ^{III} Cl ₂ (bpy) ³⁺	CH ₃ CN	3.7 ± 0.6	13 ± 2
	DMF	9.6 ± 1.3	33 ± 4
[{(bpy) ₂ Ru(dpp)} ₂ RhCl ₂] ⁵⁺	CH ₃ CN	9.4 ± 0.4	32 ± 1
	DMF	18 ± 0.7	62 ± 2

^a values shown are after 10 h of the photolysis using 470 nm LED light source (light flux = $2.36 \pm 0.05 \times 10^{19}$ photons/min; solution volume = 4.5 mL; head space volume = 15.5 ml);

^b TON = turnover number (mole of H₂ produced per mole of catalyst).

Quantum efficiency Calculation:

$$\begin{aligned} \text{quantum efficiency} &= \frac{2 \times \text{mol of H}_2 \text{ produced}}{\text{mol of photons}} \\ &= \frac{2 \times 9.8 \times 10^{-6} \text{ mol}}{2.36 \times 10^{19} \frac{\text{photons}}{\text{min}} \times 10 \text{ h} \times 60 \text{ mins} / 6.02 \times 10^{23} \text{ mol}} \\ &= 0.08\% \end{aligned}$$

References

- 1 Y. Fuchs, S. Lofters, T. Dieter, W. Shi, R. Morgan, T. C. Streckas, H. D. Gafney and A. D. Baker, *J. Am. Chem. Soc.*, 1987, **109**, 2691-2697.
- 2 A. T. Wagner, R. Zhou, K. S. Quinn, T. A. White, K. J. Brewer, *J. Phys. Chem. A.*, 2015. DOI: 10.1021/acs.jpca.5b02836 .
- 3 R Zhou, Ph.D, Dissertation, Virginia Tech, 2014.
- 4 J. V. Caspar, E. M. Kober, B. P. Sullivan and T. J. Meyer, *Inorg. Chem.*, 1982, **104**, 630-632.
- 5 S. M. Arachchige, J. Brown, R., E. Chang, A. Jain, D. F. Ziegler, K. Rangan and K. J. Brewer, *Inorg. Chem.*, 2009, **48**, 1989-2000.
- 6 T. A. White, S. M. Arachchige, B. Sedai and K. J. Brewer, *Materials*, 2010, **3**, 4328-4354.